Cuticle and Subsurface Ornamentation of Intact Plant Leaf Epidermis Under Confocal and Superresolution Microscopy

MICHAEL A. URBAN,[1] RICHARD S. BARCLAY,[2] MAYANDI SIVAGURU,[3] AND SURANGI W. PUNYASENA[1]*
[1]*Department of Plant Biology, University of Illinois, 505 South Goodwin Avenue, Urbana, Illinois 61801*
[2]*Department of Paleobiology, National Museum of Natural History, Smithsonian Institution, 10th and Constitution Avenue NW, Washington, DC 20560*
[3]*Institute for Genomic Biology, University of Illinois, 1206 West Gregory Drive, Urbana, Illinois 61801*

KEY WORDS Zeiss LSM 880 Airyscan; confocal; micromorphology; leaf epidermis; stomata

ABSTRACT Plant cuticle micromorphology is an invaluable tool in modern ecology and paleoecology. It has expanded our knowledge of systematic relationships among diverse plant groups and can be used to identify fossil plants. Furthermore, fossil plant leaf micromorphology is used for reconstructing past environments, most notably for estimating atmospheric CO_2 concentration. Here we outline a new protocol for imaging plant cuticle for archival and paleoecological applications. Traditionally, both modern reference and fossil samples undergo maceration with subsequent imaging via environmental SEM, widefield fluorescence, or light microscopy. In this paper, we demonstrate the capabilities of alternative preparation and imaging methods using confocal and superresolution microscopy with intact leaf samples. This method produces detailed three-dimensional images of surficial and subsurface structures of the intact leaf. Multiple layers are captured simultaneously, which previously required independent maceration and microtome steps. We compared clearing agents (chloral hydrate, KOH, and Visikol); mounting media (Eukitt and Hoyer's); fluorescent stains (periodic acid Schiff, propidium iodide); and confocal vs. superresolution microscopes. We conclude that Eukitt is the best medium for long-term preservation and imaging. Because of nontoxicity and ease of procurement, Visikol made for the best clearing agent. Staining improves contrast and under most circumstances PAS provided the clearest images. Supperresolution produced higher clarity images than traditional confocal, but the information gained was minimal. This new protocol provides the botanical and paleobotanical community an alternative to traditional techniques. Our proposed workflow has the net benefit of being more efficient than traditional methods, which only capture the surface of the plant epidermis. *Microsc. Res. Tech. 00:000–000, 2016.*

INTRODUCTION

The study of plant leaf micromorphology has expanded our understanding of the ecology, physiology and evolutionary relationships of plants. Micromorphological features can help to identify traits inherited as a result of shared ancestry among species, such as the t-shaped trichomes that help to define the genus *Cornus* (Dilcher, 1974). These morphological characters are integral to phylogenetic systematics, the study of the evolutionary relationships among species, but also have pharmacological applications where proper identification of the source-plant material is needed to assess the quality, and therefore the efficacy, of herbal medicines (Da Silva et al., 2015). Additionally, there are industrial uses of the study of plant cuticle morphology. A prime example is the discovery of the "lotus effect" (Barthlott, 1977), where densely packed microscale papillae protruding from the leaf create a superhydrophobic surface (Johnson and Dettre, 1964) and helps to remove particulate matter (Barthlott, 1977). The lotus effect has been co-opted for industrial applications where maintaining clean surfaces is paramount (Solga et al., 2007).

Studying the leaf epidermis has also helped us to better understand environments in deep-time (Haworth and McElwain, 2008), and as is the case for modern material, has been used in the classification and identification of fossil plants (Dilcher, 1974; Kovar-Eder et al., 2001). Multiple proxies have been developed that depend upon the interpretation of the micromorphology of leaves, including the stomatal index proxy for atmospheric CO_2 reconstruction (Beerling and Royer, 2011; Woodward, 1987), the timing of the evolution of grasses and subsequent grassland development (Strömberg, 2011), and a proxy for canopy structure that uses the correlation of epidermal cell wall shape with the widely used ecological metric, leaf area index (Dunn et al., 2015). Leaf compressions are a common component of the fossil record as far back as the Carboniferous (350 million years ago)

*Correspondence to: Surangi W. Punyasena; Department of Plant Biology, University of Illinois, 139 Morrill Hall, Urbana, IL 61801.
E-mail:punyasena@life.illinois.edu

Received 8 December 2015; accepted in revised form 19 March 2016
Review Editor: Prof. Alberto Diaspro
DOI 10.1002/jemt.22667
Published online 00 Month 2016 in Wiley Online Library (wileyonlinelibrary.com).

TABLE 1. List of specimens utilized in this study

Age	Species	Specimen #	Collection
Modern	*Ginkgo biloba*	RSB1340A	Barclay Collection
Modern	*Laurus nobilis*	US2727279	US National Herbarium
Modern	*Salix herbacea*	US1119783	US National Herbarium
Modern	*Poa sieberiana*	ILLS173962	UIUC Herbarium
Modern	*Sparattanthelium amazonum*	US1799645	US National Herbarium
Modern	*Eragrostis mexicana*	US1698021	US National Herbarium
Modern	*Oplismenus hirtellus*	ILLS191872	UIUC Herbarium
Modern	*Taxodium distichum*	US3662427	US National Herbarium
Modern	*Picea sitchensis*	US3520419	US National Herbarium
Early Eocene[a]	*Ginkgo adiantoides*	USNM617420	US National Museum
Late Cretaceous[b]	*Ginkgo adiantoides*	USNM617419	US National Museum

[a]56 million years old—Willwood Formation, Nebraska.
[b]66 million years old—Hells Creek Formation, Wyoming.

(Willis and McElwain, 2013). The details of the leaf surface are fundamental to the identification and classification of these extinct plant forms (Cleal and Zodrow, 1989).

Despite the unique information that the leaf epidermis provides about modern and paleoenvironments, morphological studies of the leaf epidermis have lagged other botanical pursuits. This is primarily because preparing and analyzing leaf material is time consuming. Plant specimens must be macerated, cleared, stained, and mounted on permanent glass slides in order to study the details and capture them as images (Dilcher, 1974). This process takes many months and despite large efforts produces only small datasets. Also, storing physical slide collections in perpetuity can be costly and arguably not worthwhile. In just a few decades, some mounting media can recrystallize and develop autofluorescence not present when originally prepared (e.g., in <10 years for Coverbond mounting medium; Feldman and Dapson, 1981).

It is sometimes possible to unmount specimens, the preferred option when leaf material is irreplaceable, as is the case for historical collections from herbaria and fossil material in natural history collections. However, in many cases, it is more effective to start over with fresh material. Thus, many prepared leaf collections intentionally developed as long-term comparative databases are now of limited use. The efforts of each scientific generation must be redone by subsequent generations. Photographing these archives of glass-slide mounted leaf specimens has been a stop-gap measure to preserve the collections in their present state (Barclay et al., 2007), and the creation of online databases of these images, (e.g., the cuticle database; Barclay et al., 2012) have served to broaden the reach of these collections. However, the original preparation technique often eliminates fluorescence properties, limiting subsequent investigation to transmitted light microscopy.

In this paper, we outline a methodology that addresses many of the current limitations of cuticle preparation and imaging. We prepare the leaves intact, imaging them with superresolution and confocal microscopy. Our preparation methods build upon existing technologies and practices, but are a unique combination of approaches that increase the rate of data collection and create physically more robust specimens that are easier to manipulate. Also, the use of confocal microscopy with Airyscan technology described in this study allows for high-resolution digital preservation of leaf material, by producing 3D point-cloud datasets that can subsequently be reinvestigated and reinterpreted by later generations of scientists. With these Airyscan images, the surface features of the epidermis can be studied in great detail, and simultaneously, the internal anatomy of the leaf can be studied at multiple planes, previously only possible through tedious and difficult microtome procedures. An additional benefit is that our techniques are applicable to both modern and fossil material. This allows for a direct comparison and avoids artifacts that may arise from the need to prepare modern and fossil material differently.

MATERIALS AND METHODS

Origin and Preparation of Modern and Fossil Plant Specimens

Modern plant specimens were collected from herbarium sheets at the United States National Herbarium (US—Smithsonian Institution) and the University of Illinois Herbarium (ILL, Table 1). Leaf material was removed from the herbarium sheets, and 2 × 2 mm subsamples were cut using a basic scalpel. Whip grasses like *Poa sieberiana* and conifer needles (e.g., *Taxodium distichum*) were cut at 2–3 mm lengths.

Small sheets of fossil cuticle were extracted from the rock sample surface using tweezers, and cleaned with paint brushes to remove any adhering sediment. The fossil specimens of *Ginkgo adiantoides* studied here came from two different geologic formations. The Late Cretaceous material (66 Ma) was collected from the "Skunk Hunt" fossil plant locality in the Hell Creek Formation of Southwestern North Dakota (Loc. KJ1305; USNM617419, US National Museum). The Hell Creek material was removed from rock specimens with tweezers, and because it was already dry and the surface was clean of sediment, it was mounted without further treatment. The early Eocene-aged specimens (56 Ma) came from the "Ants Steal Cuticle" locality in the Willwood Formation of Wyoming (Loc. SLW0907; USNM617420). These were more firmly adhered to the rock, and thus were "peeled" off the rock using the polyester overlay technique adhering the upper leaf surface to the overlay, leaving the lower surface exposed (Kouwenberg et al., 2007). Silicate minerals were removed by immersing the fossil + overlay in concentrated hydrofluoric acid overnight. The fossil-+ overlay was neutralized by dilution in DI water, and

air-dried before mounting. *Ginkgo biloba* was selected as our primary study organism for comparison, given its prominence as a paleoenvironmental proxy. The epidermal morphology of the genus has remained relatively unchanged since the Late Cretaceous, and *G. biloba* has often been used as a modern analog species to reconstruct atmospheric CO_2 (pCO_2) in deep time (e.g., Barclay and Wing, 2016; Beerling et al., 1998; Kürschner et al., 2008).

Clearing Procedure

Cuticles specimens were wetted with a 5% solution of Triton X-100 (Fisher Scientific, Pittsburgh) in a 5 mL plastic centrifuge tube for 24 h in order to hydrate the dried plant material. Triton X acts as a surfactant increasing the efficiency of wetting. In this study, we compared three different clearing agents to assess which would be most effective in producing quality images: chloral hydrate, Visikol, and potassium hydroxide. Chloral hydrate (2.5 g chloral hydrate: 1 mL 30% glycerol) is a classic tool for clearing plant tissues (Berleth, 1993). However, it is a class IV controlled substance in the United States, making procurement difficult for labs that do not have the proper license to purchase and store the chemical (access for this study was provided by the DEA License maintained by Mayandi Sivaguru). Visikol (Phytosys, Somerville) is a relatively new alternative to chloral hydrate that uses a proprietary formula that promises to be equivalent to chloral hydrate, yet is readily available without the need for special permits (Villani et al., 2013). A 10% solution of potassium hydroxide (KOH) was also tested because it is a quick-acting clearing agent often used on bryophytes and other plants (Glime and Wagner, 2013), and is also inexpensive and easy to obtain. For chloral hydrate and Visikol preparations, the leaf samples were incubated in the clearing agents for 3–24 h until they started to appear transparent. Thicker leaves and needles tended to require additional clearing time. Visikol immersed samples were also placed on a hotplate at 40°C to decrease clearing time. For KOH, samples were immersed in the 10% solution and placed in a hot bath for 15–20 min set at ~90°C.

Staining Procedure

After clearing, cuticle samples were washed with distilled water several times before being stained with periodic acid and Schiff's reagent (PAS; Sigma-Aldrich, Allentown, PA), propidium iodide (PI; Life Technologies, Eugene, OR), or a mixture of PAS + PI. For PAS, we followed the kit manufacturer's protocol. PAS is known to label aldehydes and glycogen in animal tissues (Sivaguru et al., 2015). Cuticle samples were immersed in periodic acid for 30–45 min followed by three washes in distilled water. The samples were then stained with Schiff's reagent for a minimum of 15 min or until the center of the samples turned a faint purple in color. The Schiff's reagent tended to form noticeable crystals in the bottle, so was filtered through a 10 μm cell strainer to remove the crystals before being applied to the leaf. The samples were then washed several times in DI water until the color fully developed via oxidation, and all excess stain in the solution was removed. For PI, the samples were immersed in a 1 μL/mL solution for 30 min. They were then washed in distilled water to remove excess dye. The dual stained samples were stained with PAS first and then PI. Staining order had no effect on the final results.

Mounting Procedures

The stained cuticle was mounted in either Hoyer's medium or Eukitt quick mounting medium (O. Kindler GmbH, Freiburg, Germany). Hoyer's medium (refractive index = 1.531) is a glycerin/chloral hydrate based medium and was created using 50 mL water, 30 g gum arabic, 200 g chloral hydrate and 20 mL glycerin as originally formulated (Anderson, 1954). Eukitt is a proprietary resin-based medium dissolved in xylene (refractive index = 1.533). Before mounting, samples were dehydrated in a graded ethanol series for Hoyer's (70, 80, and 100% ethanol) or a graded isopropanol/xylene series for Eukitt (70, 80, and 100% isopropanol followed by 2:1, 1:1, and 1:2 isopropanol/xylene before finally 100% xylene). Mounting medium was applied to a 24 × 40 mm coverslip (0.17 mm thick) with a disposable pipette, and the samples were placed on top. Two to three drops of the medium were then applied over the sample and a high performance 22 × 22 mm cover glass (0.17 mm thick). Mounting with two coverslips allowed us to image both sides of the leaf. The samples mounted in Hoyer's solution were left to harden for 2 weeks in a ventilation hood. Samples mounted in Eukitt were dried overnight.

Imaging Cuticle Using eSEM

For our electron micrographs, dried leaves were macerated using a three step chemical process to separate them into upper and lower cuticles (Barclay and Wing, 2016). Samples were soaked in DI water for 24 h, replaced with dilute HCl (5% v/v) for at least 1 day (ideally 2 days) to prevent fungal and algal growth on the leaf surface and to increase the efficiency of maceration. Samples were rinsed three times to neutralize the HCl, and placed into 20 mL of a 25% solution (w/v) of chromium trioxide [$Cr(VI)O_3$].

Cuticle specimens were mounted onto 12 mm scanning electron microscope (SEM) stubs, adhered to carbon-conductive double-sided adhesive discs (SPI#05077-BA), under an Olympus SZX12 binocular microscope at 160× magnification, placed with the internal side facing upwards, and then air-dried. Uncoated specimens were imaged under low vacuum (32 Pa) in a Carl Zeiss EVO-MA15 environmental SEM (eSEM) in the SEM lab of the Smithsonian National Museum of Natural History in Washington D.C. The voltage target was 15 kV, with an ion probe set at 900 pA, and a working distance of 8–10 mm. Images were created using only the top two backscatter detectors to create shadows and highlight microtopography.

Imaging Cuticle Using Confocal and Airyscan Superresolution Microscopes

We used the LSM 880 with Airyscan (Carl Zeiss, Jena, Germany) system with GaAsP detectors (Gallium:Arsenide:Phosphide) for both confocal and Airyscan imaging (Table 2). The Airyscan represents a new confocal imaging technique that provides a twofold

TABLE 2. Description of optical techniques and methods used to produce images of intact plant leaf cuticle

	Confocal (GaAsP)	Airyscan
Systems	LSM 880, Carl Zeiss, Jena, Germany	LSM 880, Carl Zeiss, Jena, Germany
Objectives	25× Plan Apochromat/0.8 lmm Korr DIC M27, 40x C-Apochromat/1.2 W Korr FCS M27	25× Plan Apochromat/0.8 lmm Korr DIC M27, 40× C-Apochromat/1.2 W Korr FCS M27
Dimensions (*X*, *Y*, *Z* in μm)	1024 × 1024 (0.04 × 0.04 × 0.1)	1024 × 1024 (0.04 × 0.04 × 0.1)
Emission wavelengths	Ex488 − Em495-550 + LP 570; Ex561 − Em 570-620 + LP 750	Ex488 − Em495-550 + LP 570; Ex561 − Em 570-620 + LP 750
Excitation wavelengths	488 nm, 561 nm	488 nm, 561 nm
Detectors	Airyscan detector (Confocal Mode)	Airyscan detector (Airyscan Mode)
Digital postprocessing and software	Subset of processed data planes, Max intensity projection, 3 × 3 median filter-Zen	Airyscan module, Subset of processed data planes, Max intensity projection, 3 × 3 median filter—Zen

improvement in the signal:noise ratio (SNR) over conventional detectors (Weisshart, 2014). In both modes, a 25× Plan Apochromat (1.4NA) long working distance oil objective was used. In the confocal mode, the master pinhole was set to 1.0 airy unit (AU), a measure of pinhole size, and in the Airyscan mode it is set at 1.25 AU. We used the same GaAsP detectors in both Airyscan and confocal modes. In the Airyscan superresolution mode, emission light from every pixel is projected onto 32 honeycomb-shaped hexagonal GaAsP detectors (each representing 0.2AU; Weisshart, 2014), arranged in three rings with a central detector. In the standard confocal approach, only one detector is used. With Airyscan, there is a maximum of six detectors at any given position. This results in more light collected than by a standard confocal. The collected photons for each pixel are re-assigned to the center pixel after averaging the intensity in each ring of detectors. This produces an image that is ∼1.4× higher resolution (170 nm) than the diffraction limit of light (220 nm). Since the point spread function is known for each of the 32 detectors used, the signal to noise is improved by performing an additional 3D deconvolution step together with a Wiener filter (Weisshart, 2014). The final result is a 1.7× improvement in resolution over the diffraction limit. The confocal and Airyscan image acquisition settings are provided in Table 2.

A series of images were taken at 1.0 μm steps in the Z direction to produce a "Z stack". The raw and processed (confocal and Airyscan) images were saved in the CZI format utilized by the Zeiss Zen software. Maximum intensity projections and orthogonal sections were produced for each image within the Zen software package.

RESULTS

In Figure 1, we present a comparison of *G. biloba* imaged with both the eSEM (Figs. 1A and 1B) and LSM 880 Airyscan (superresolution) (Figs. 1C and 1D). The leaf surfaces presented in Figures 1A–1D were macerated in the same manner to separate the adaxial (upper) from the abaxial (lower) layer of the plant leaf. The inside and outside of the abaxial cuticle were then imaged. In the Airyscan images of the macerated *G. biloba* leaf (Figs. 1C and 1D), the leaf has only been mounted in Hoyer's medium without any further treatment. The three-dimensional structure of papillae and the shape and size of the guard cells are readily apparent in these images; however, the low contrast leads to difficulty in identifying the epidermal cell walls or their arrangement.

With sufficient clearing and the introduction of fluorescent staining for increased contrast, it is possible to use intact leaves to produce eSEM quality images of multiple planes with Airyscan. An example of this can be seen in Figure 1E. In Figure 1E, *G. biloba* is cleared with chloral hydrate and stained with PAS (a cellulose stain), and mounted in Hoyer's medium. The combination of clearing and staining produces an image on par with that of the eSEM (Figs. 1A and 1B), with the high contrast that is missing from the unstained sample (Figs. 1C and 1D). The depth of penetration of the orthogonal cross section (top of Fig. 1E) reveals not only structure of the epidermal and deeper parenchyma cells, but also the thickness of the waxy coating of the epidermis and size and depth of stomatal openings. The depth of the stomatal pore is an important variable when using models to reconstruct pCO_2 (Roth-Nebelsick et al., 2014), and is impossible to measure using SEM and transmitted light without first creating microtome thin sections after embedding the specimen in wax.

Though we present an optimal example of Airyscan imaging in Figure 1E, it was first important to identify the preparation techniques that produced the best images while still providing a potential long term physical archive that could be produced in a reasonable amount of time. In Figures 2 and 3, we try a number of combinations of clearing agents (chloral hydrate, Visikol, and potassium hydroxide), several common stains (PAS, PI, PAS + PI), and two mounting media (Eukitt, Hoyer's).

The mounting medium (Fig. 2) proved to be the first challenge. Hoyer's belongs to a group of "gum-chloral" mounting media that have been traditionally used to mount arthropod, bryophyte, and other plant specimens (e.g., Brown, 1997). It has the benefit of continued clearing after mounting (from the chloral hydrate) but this could be problematic for stained specimens. Hoyer's medium tended to "leach" the stain from the samples over time, producing a purple/red halo around the specimen. The effect tended to worsen as the slides aged. The effect results in a slight autofluorescence of the medium when imaged with Airyscan and confocal. This is apparent in the orthogonal cross sections in Figures 2A, 2C, and 2E. The area above the leaf tends to be brighter than the complete black of the samples mounted in Eukitt (Figs. 2B, 2D, and 2F). A more extreme example can be found in Figure 4A (*Laurus nobilis*). However, the fluorescence of the stain within the medium is only an issue if the intensity becomes greater than that of the cuticle itself. Furthermore,

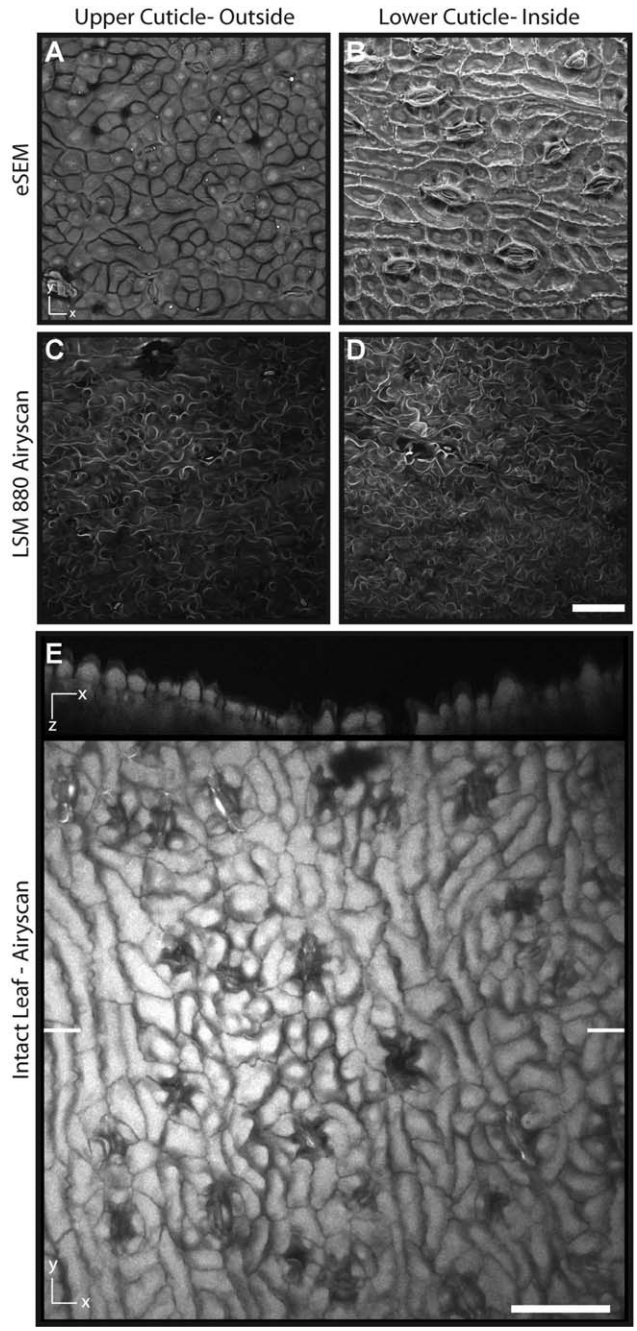

Fig. 1. Comparison of intact imaging of plant leaves versus traditional maceration and imaging with a scanning electron microscope. All images are of *Ginkgo biloba*, but are not from the same sample. (A, B) Uncoated and unstained environmental SEM images of *G. biloba* macerated with $Cr(VI)O_3$ to separate the upper and lower cuticle. (C, D) Maximum intensity projections of unstained and uncleared images of *G. biloba* macerated with $Cr(VI)O_3$ imaged using the Zeiss LSM 880 in Airyscan mode. (E) Maximum intensity projection image of intact leaf (upper and lower cuticles kept together). Leaf was cleared with chloral hydrate, stained with periodic acid-Schiff, mounted using Hoyer's solution, and then imaged with the Zeiss LSM 880 in Airyscan mode. The intact leaf simultaneously reveals both the external epidermal morphology and the subsurface cell wall outlines. Scale bar in D applies to A–D. White tick marks on the sides of (E) represent the location of the orthogonal projection presented at the top. All scale bars 10 μm.

Hoyer's can take weeks to fully harden for thicker cuticle mounts (because more medium is required), making the manipulation of the double-sided slides difficult in the short term. Hoyer's also can recrystallize when exposed to humid conditions, which makes its long-term stability uncertain. Chloral hydrate, a primary component of Hoyer's, is also difficult to procure in the United States due to its classification as a controlled substance. Finally, the medium itself can be difficult to consistently mix in the lab.

For these reasons, Eukitt, though a proprietary medium, is likely the superior mounting medium for both imaging and long-term stability. Specimens embedded in Eukitt produce high resolution images (Figs. 1B, 1D, and 1F) and it can be easily purchased ready-made, an advantage because this results in a more uniform and standard composition than Hoyer's, which is mixed as needed and will vary slightly between batches. Eukitt typically takes only a few hours to dry to a glass-like resin, which the manufacturer claims will remain stable for decades. However, like most resin-based media the samples must be dehydrated into 100% xylene, which is a highly volatile carcinogen. Mounting in Eukitt requires a well-ventilated hood.

In our comparison of clearing agents, the differences between chloral hydrate and Visikol were difficult to discern, but this was expected given that Visikol was expressly developed as a replacement for chloral hydrate (Villani et al., 2013). Visikol took 2–3 times longer to clear tissue, but otherwise the preparation was the same. Potassium hydroxide (KOH), however, provided inconsistent results during preparation. KOH and similar oxidizing agents used in clearing (e.g., sodium hypochlorite or Schultz's solution) are caustic and potentially damage the leaf during clearing. The sensitivity of a sample was somewhat dependent upon the thickness of the cuticle. It took the least amount of time to clear (~15–20 min), but it made the leaf fragile and difficult to manipulate while mounting. In our experiments, longer incubation times in KOH damaged the more delicate specimens. As shown in the orthogonal images in Figures 2E and 2F, KOH appears to remove intracellular material. Only the cell walls remain, which may make it the optimal choice if the isolation of cell walls is the scientific objective.

In Figure 3, we compared two common stains (PAS, PI) along with their dual application to discern which would produce the best images of *G. biloba* cuticle using the superresolution Airyscan and confocal modes of the LSM 880. The visible difference between Airyscan and confocal images was minimal for the size of structures we examined (magnification of 250×). The two modalities could potentially be used interchangeably. However, Airyscan still has 1.7× higher resolution than confocal and would be preferable if available, especially at higher magnification. The confocal images also appear to be slightly brighter on average, but this relates little to clarity in differentiating structures, and images from a traditional confocal could be further improved during postprocessing with most microscope software.

Overall, the benefit of staining can be ascertained by comparing the unstained cuticle in Figures 3G and 3H with the stained images in Figures 3A–3F. It is

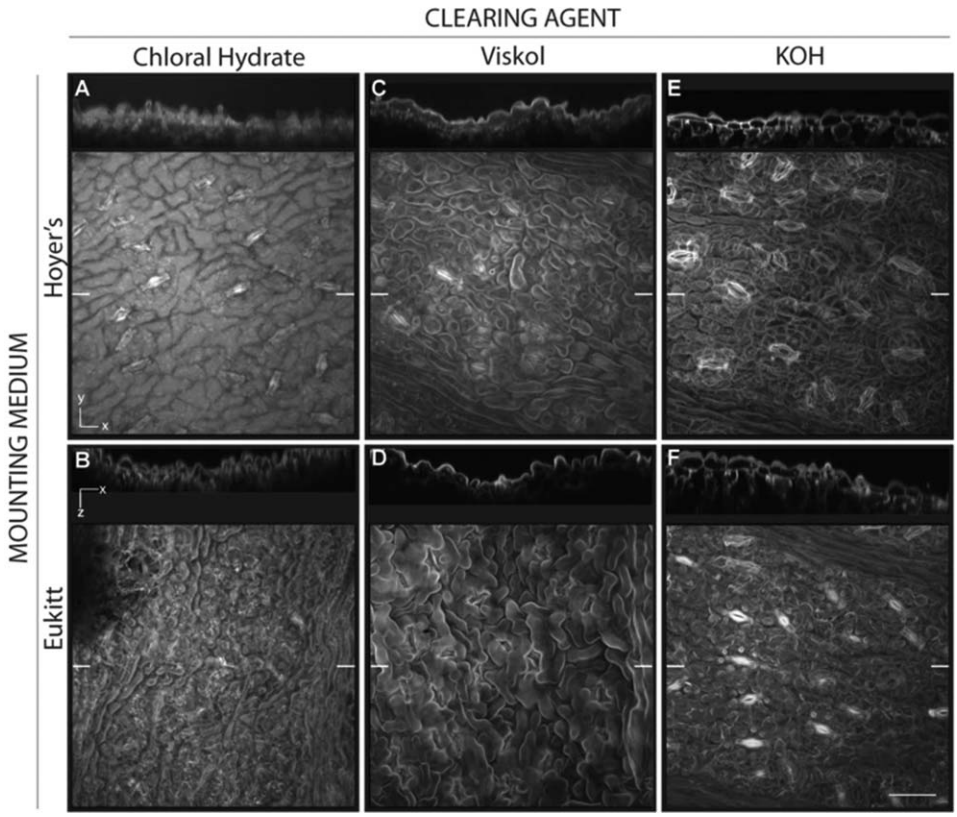

Fig. 2. Comparison of clearing chemicals and mounting media using *Ginkgo biloba* as our model. All samples were stained with PAS + PI. Samples cleared with either chloral hydrate (A, B), Viskol (C, D), or potassium hydroxide (E, F), and then mounted in either Hoyer's solution (A–C) or Eukitt (B–F). Sample number RSB1340A [Barclay collection on Library or Congress Grounds in Washington, D.C.]. White tickmarks on edges designate location of orthogonal projection. Scale bar in (F) is 10 μm and applies to all images.

possible to produce a high-quality image without staining (if the material is naturally autofluorescent), but the contrast in the images makes it more difficult to identify cell wall structure and the position, number, and size of papillae. The guard cells of the stomata are still very clear regardless of staining. Propidium iodide (PI) is often used to stain nuclear material and cytoplasm and can be used to assess cell viability (Jones et al., 1985). In cells with intact plasma membranes PI is excluded. Our herbarium samples were dried years ago, thus the PI stain is able to enter the cells producing a red label. In Figures 3A and 3B, the PI produces images emphasizing the cells while leaving the cell walls unstained and black. For *G. biloba* this appears to make it difficult to see the papillae around the stomata. PAS is a cellulose stain that is useful for looking at cell walls (Ruzin, 1999). Polysaccharides in cellulose react with the stain producing a deep magenta color. In Figures 3C and 3D, this produces a much clearer three-dimensional image than with PI alone. The papillae and other structures are easy to discern, although these may obscure the underlying epidermal cell arrangement visible in the PI images. The combination of stains produce images very similar to that of PAS alone making it usually unnecessary to stain with both PAS and PI. However, a combination of both PAS and PI does appear to slightly increase the contrast in some samples where they been applied. In Figures 3E and 3F, the edges of the papillae appear to be slightly better defined than in Figures 3C and 3D, but the benefit of using both stains is minimal. Although all of these images were taken using the same leaf, it should be noted that there is some variability in cuticle structure within a single leaf. However, the actual diagnostic features such as veinal areas or stomatal structure remain unchanged despite minor visual differences.

Figure 4 shows that our preparation and imaging techniques can be applied to a diverse group of plant species, including dicot and monocot angiosperms, as well as gymnosperms. We found that the best preparation technique for each species varied tremendously (details for the preparation technique and imaging method used are provided in the figure caption of Fig. 4). When the most appropriate combination is achieved, the final preparation highlights typical epidermal features such as stomata (gas-exchange pores), trichomes (hair cells), papillae (epidermis extensions), and cell wall patterns. KOH was the most effective at isolating cell walls, but can be a harsh treatment, with Visikol and chloral hydrate producing workable results for a number of species (e.g., *Sparattanthelium amazonia, Salix herbacea*). PAS overall seems to be the best choice of stain for most species. However, PI can also at times produce near SEM quality (Palmer and Tucker, 1981) images for grasses (Figs. 4D–4F). The mounting media (Hoyer's and Eukitt) were largely

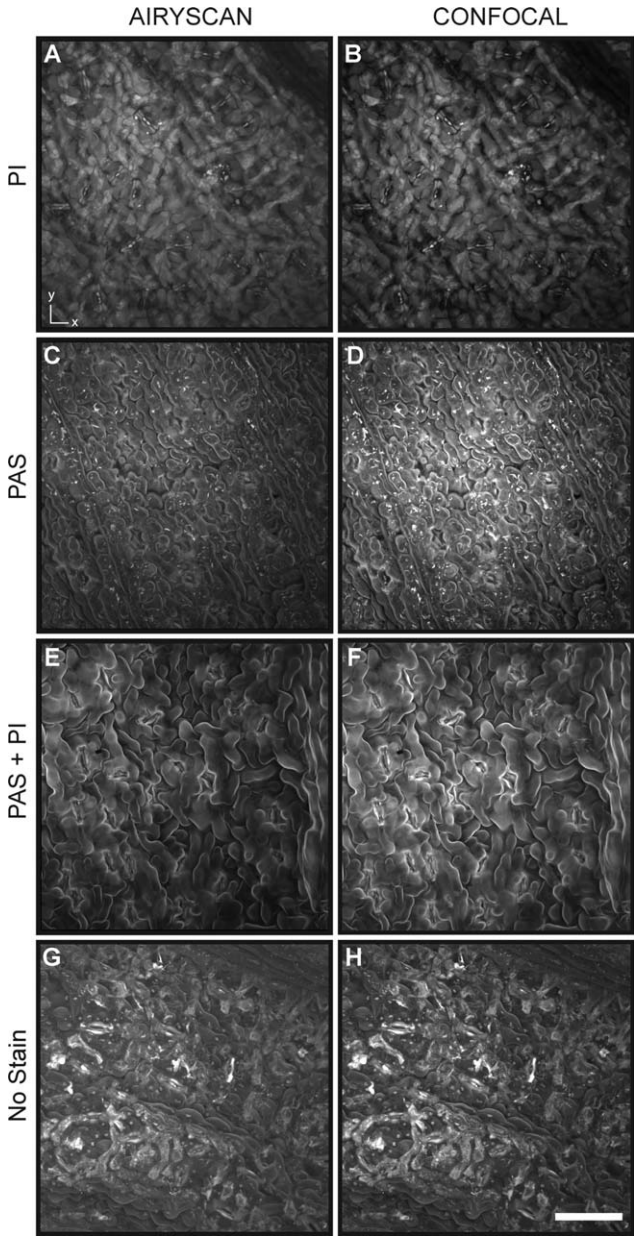

Fig. 3. Results of intact leaf staining on *Ginkgo biloba* (RSB1340A). (A, B) Propidium iodide (PI); (C, D) periodic acid Schiff (PAS); (E, F) periodic acid-Schiff mixed with propidium iodide (PAS + PI); and (G, H) control specimen imaged without stain. All specimens cleared with chloral hydrate (CH) and mounted with Eukitt. Scale bar in (H) is 10 μm and applies to all images.

interchangeable, affecting image quality only when "stain bleed" was strong. An almost equal number of species were imaged as well by traditional confocal as with Airyscan, but the increased resolution of Airyscan is more critical at higher magnification.

Ultimately, we want to apply our techniques to fossil samples. In Figure 5, we present fossilized cuticle of *G. adiantoides* from the Late Cretaceous (66 Ma) and early Eocene (56 Ma). The fossilized cuticle was not cleared or stained. It was directly mounted in Eukitt because the material naturally fluoresces. With only a thin portion of the epidermis remaining, the fossil cuticle has the benefit of not having any extraneous organic material that could potentially affect imaging quality. The results highlighted in Figure 5 demonstrate the importance of the microscopy method used. The high-resolution Airyscan (Figs. 5A–5F, 5J) produced superior images to widefield fluorescence, the standard approach to imaging fossil material (Figs. 5G–5I).

DISCUSSION

Our study explores multiple preparation and imaging techniques that are conducive to the archival preservation of modern plant cuticle in reference collections (Barclay et al., 2007, 2012) and for paleoenvironmental studies based upon plant cuticle (e.g., Lomax and Fraser, 2015; Roth-Nebelsick, 2005; Wooller et al., 2003). A summary of our preparation and imaging techniques is outlined in a flowchart (Fig. 6). In the standard approach to cuticle analysis, leaves are macerated to separate the upper and lower cuticles using aqueous oxidizing agents (e.g., sodium hypochlorite, $Cr(VI)O_3$, Schultz's solution; Kouwenberg et al., 2007), then stained with safranin O, bismuth brown, or toluidine blue, and then mounted on glass slides for transmitted light microscopy (Dilcher, 1974). Another common method is the use of scanning electron microcopy (SEM), a destructive approach where the leaves are similarly macerated, but then permanently mounted on stubs for imaging (Barclay and Wing, 2016; Stockey and Frevel, 1997; Stockey et al., 1998). Both techniques are time consuming, making the creation of the large datasets needed for paleoenvironmental studies nearly unfeasible. From initial preparation to imaging, it can take up to 5 days and ~2 h of hands-on time to prepare and image one sample. Furthermore, the maceration of the leaf can lead to unintended damage to the subsurface features of the leaves.

Superresolution (Airyscan) and confocal microscopy of intact leaves have the potential to produce images of microstructures on plant leaves at a resolution comparable to that of SEM, without requiring maceration. In some cases, the imaging can be superior to an SEM, by allowing the visualization of morphology below the surface of the cuticle. Our methods using the intact leaves reduces the total time for preparation and imaging by at least 2 days and total hands-on time by one third (~135 min vs. ~90 min.). Fossil specimens can be even less time-intensive (e.g., *G. adiantoides* in Fig. 5), ready for imaging in a few hours. Fossil cuticle is sometimes only loosely adhered to the rock and can be removed with tweezers. The fossil is often naturally fluorescent, and if clean of sediment, does not require further processing (as was the case for our Late Cretaceous *G. adiantoides* material; Figs. 5D–5F). Dehydration is not required, which eliminates the possibility of shrinkage effects caused by solvents (Cleal and Shute, 2007). The fossil leaf can be immediately mounted in Eukitt and can be ready for imaging within 2–4 h of mounting. Our early Eocene fossil material required chemical cleaning (see "Methods"), which added more preparation time, but once cleaned and dried, was mounted and quickly ready for imaging.

Modern material requires clearing and staining. Visikol and chloral hydrate penetrated to a similar depth

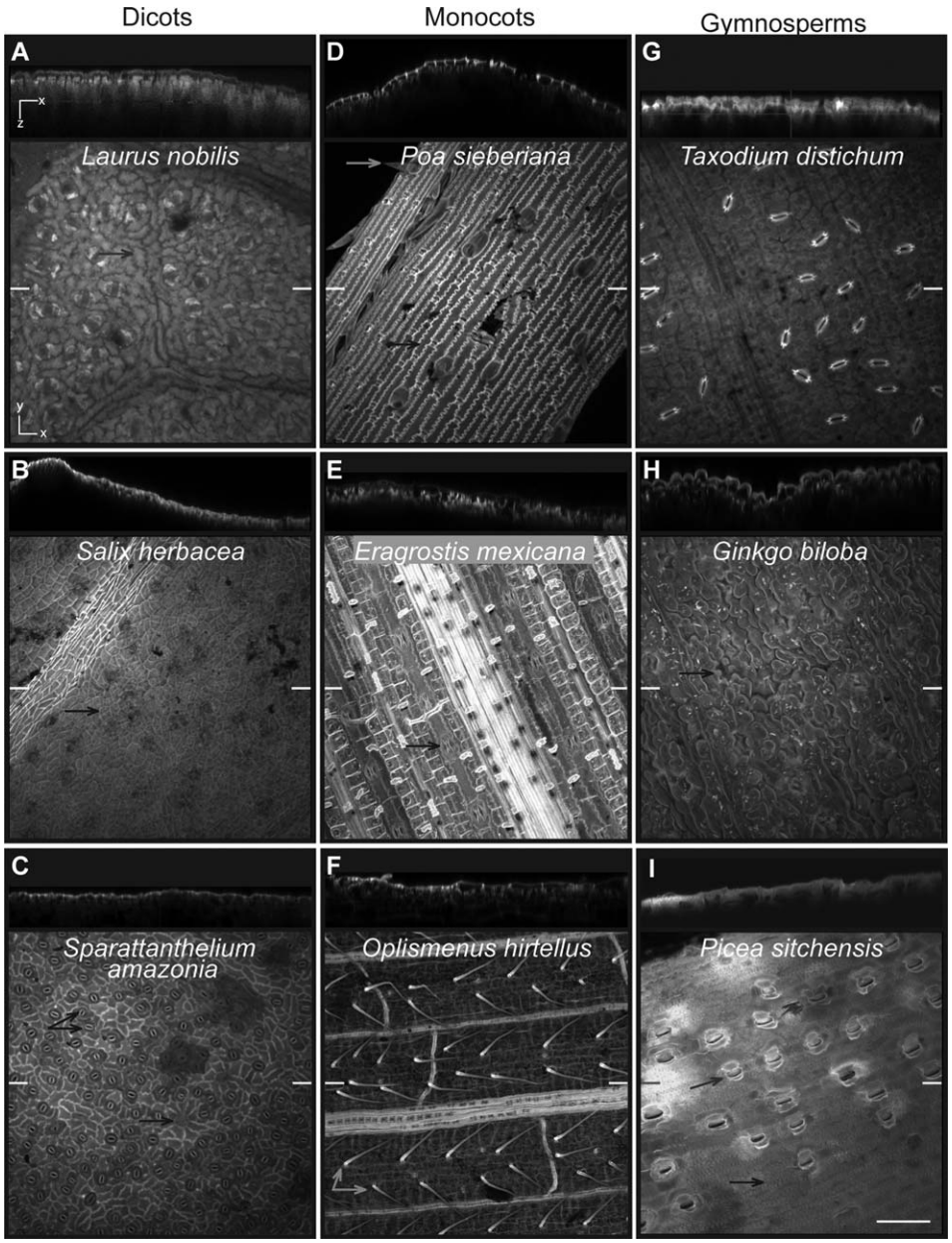

Fig. 4. Maximum intensity projection images from a broad taxonomic range of vascular plant species. White tickmarks on edges designate location of orthogonal projection. Arrows indicate important features. Scale bar in (I) is 10 μm and applies to all images. (A) *Laurus nobilis* L. (US2727279), CH/PAS + PI/Hoyer's/Airyscan, Arrow: undulating boundaries between epidermal cells, (B) *Salix herbacea* L. (US1119783), Visikol/PAS/Eukitt/Airyscan, arrow: straight cell walls; (C) *Sparattanthelium amazonum* Mart. (US1799645), KOH/PAS/Eukitt/Airyscan, Arrows: kidney bean shaped guard-cells (top), trichome base (bottom); (D) *Poa sieberiana* Spreng. (ILLS173962), Visikol/PAS/Eukitt/confocal, arrows: trichrome (top), rectangular cell walls (bottom); (E) *Eragrostis mexicana* (Hornem.) Link (US1698021), KOH/PI/Eukitt/confocal, arrow: dumbbell shaped stomata ; (F) *Oplismenus hirtellus* (L.) P.Beauv. (ILLS191872), KOH/PI/Hoyer's/Confocal; (G) *Taxodium distichum* (L.) Rich. (US3662427), CH/PAS + PI/Hoyer's/confocal; (H) *Ginkgo biloba* L. (RSB1340A, Barclay collection), Visikol/PAS/Hoyer's/Airyscan, arrow: papillae; (I) *Picea sitchensis* (Bong.) Carrière (US3520419), KOH/PAS/Eukitt/Airyscan. 279 × 361 mm (300 × 300 DPI), arrows: kidney bean shaped guardcells (top), rectangular cell walls (bottom).

within the leaf mesophyll (Figs. 2A–2D). Both were equally easy to use, which leaves the choice up to the laboratory. KOH effectively cleared the samples (Figs. 2E and 2F). However, for delicate samples, KOH can macerate the mesophyll tissues, separating upper and lower cuticles, or the leaf can become weakened, making further handling difficult. The duration of incubation varied for leaves and needles of different thicknesses. Long incubation periods could result in potential deterioration of the leaves. Thus, careful attention to the process or experimentation is required in advance of final preps. The longer incubation times of Visikol and chloral hydrate did not appear to damage the plant tissue. The natural fluorescence of the intact plant leaf provided an inadequate view of features on the surface and subsurface (Figs. 3G and 3H).

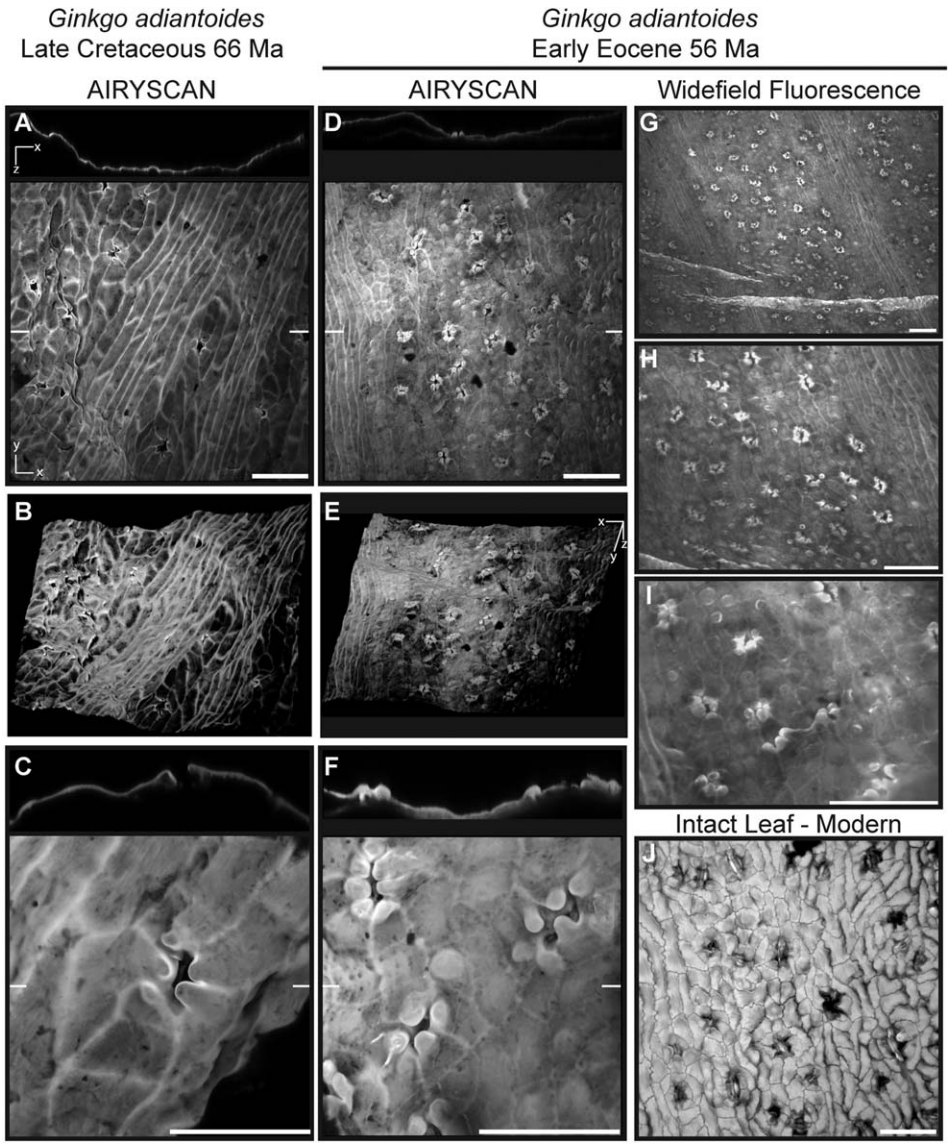

Fig. 5. Airyscan images of fossil *Ginkgo adiantoides* from the Late Cretaceous and Early Eocene compared with images taken of the same specimens using traditional widefield fluorescence. (A–C) *G. adiantoides* from the Late Cretaceous (66 Ma) Hell Creek formation (USNM617419) with (A) 25× magnification, (B) three-dimensional surface image at 25×, and (C) a 63× magnification image of individual stomata. (D–I) *G. adiantoides* from the Early Eocene (56 Ma) Willwood Formation (USNM617420). (J) Intact leaf of modern *Ginkgo biloba* imaged with Airyscan included to compare with the fossil material (RSB1273). White tickmarks on edges designate location of orthogonal projection. All scale bars 100 μm.

We found that PAS or a combination of PAS + PI stains worked the best at revealing relevant diagnostic features of the surface and subsurface anatomy.

Eukitt provided a number of advantages over Hoyer's mounting medium beyond the ease of procurement. Initially, there did not appear to be much difference in the image quality (Fig. 2). However, the chloral hydrate in Hoyer's continued to clear the specimens over time, often leading to "bleeding" of stain into the mounting medium. At first, fluorescence in the medium did little to affect the contrast for the specimens, as seen in the slight haziness of the orthogonal image in Figure 2A, but the contrast decreased over time resulting in loss of depth of penetration and clarity in maximum intensity projections. Also, Hoyer's took weeks (or months for several samples) to fully dry for thicker specimens, particularly for the conifer needles we studied. The slides then needed to be ringed with wax to prevent recrystallization due to ambient humidity. Eukitt solidified into a glass-like resin in hours and did not require a ring of wax sealant around the cover glass. If long-term storage is not a priority, then the mounting properties of Hoyer's medium are more than adequate. However, we recommend mounting samples using Eukitt because it is easier to use and potentially stable for decades, which makes it the better choice for archival preservation.

Our results illustrate the taxonomic breadth to which our imaging and mounting techniques can be applied: eudicot angiosperms, monocot angiosperms, and gymnosperms. Each species reacted differently to

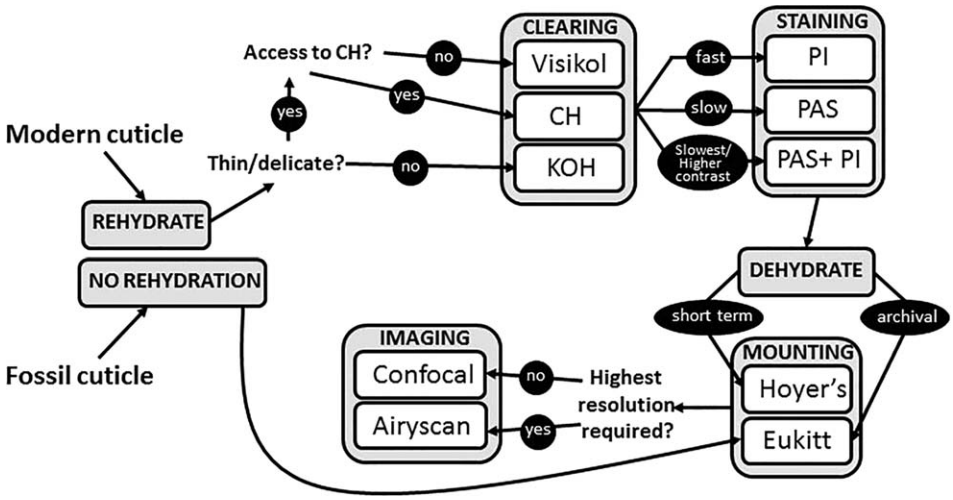

Fig. 6. Flowchart detailing the summary of steps for preparing and imaging options for various types of cuticle samples. Access to chloral hydrate refers to its status as a schedule IV controlled substance in the United States. CH: chloral hydrate, PI: propidium iodide, PAS: periodic acid Schiff, KOH: potassium hydroxide.

the various preparation treatments, so the images in Figure 4 represent the combination of preparation and imaging techniques that produced the best final product. The differential response of the leaves to different treatments was likely due to inherent differences in leaf structure and anatomy of the diverse groups of species we studied. No single combination of clearing agents and stains always created the best preparation, which required experimenting using multiple combinations in parallel until the best combination was achieved. We found that by using the full suite of preparation techniques outlined here that it was possible to obtain high quality images for all taxonomic groups.

Our techniques allowed us to isolate and image numerous surface and subsurface features of the leaf epidermis that are used to identify the major taxonomic groups of terrestrial plants. One diagnostic characteristic is cell shape. We readily imaged the two major types of guard cell structures. The majority of vascular plants have stomatal pores bounded by kidney-bean-shaped guard cells (Figs. 4A–4C), but *Eragrostis mexicana* has dumbbell-shaped guard cells (Fig. 4E), a recently evolved diagnostic feature of grasses. Cell wall boundaries in dicots are most commonly shaped as polygons, either straight as in *S. herbacea* (Fig. 4B) or rounded as in *S. amazonia* (Fig. 4C). In contrast, monocots like *P. sieberiana* (Fig. 4D) and gymnosperms such as *Picea sitchensis* (Fig. 4I) have more rectangular cell wall boundaries. Another diagnostic characteristic is cell arrangement. The arrangement of stomata aligned into rows is typical of most gymnosperms (Figs. 4G and 4I), but it is also common for the grass family, as in *P. sieberiana* and *E. mexicana* (Figs. 4D and 4E). However, *T. distichum* (Fig. 4G) shows that this is not a rigid rule for all conifers. We also able to image the unique characters of *G. biloba* (Fig. 4H). *G. biloba* has the parallel veins typical of many gymnosperms in addition to veins that bifurcate in the same way as ferns. Moreover, *G. biloba* is unique in having stomata that are both randomly dispersed and oriented in non-veinal areas, a feature more common in angiosperms like *S. herbacea* (Fig. 4B) and *S. amazonia* (Fig. 4C).

Other epidermal features, when present, may provide useful taxonomic information, but some may also be influenced by environmental factors that modify their number, position, or aspect (Barclay et al., 2007). The frequency of stomata on the leaf surface is influenced by atmospheric CO_2 concentration (Woodward, 1987), and is utilized as a proxy for atmospheric CO_2 on the scale of thousands to millions of years (Kürschner et al., 2008; Retallack, 2001; Van der Burgh et al., 1993). *G. biloba* is often used as a calibration species to quantify changes to CO_2 in deep time (Fig. 1E, Figs. 2 and 3; Barclay and Wing, 2016). Trichomes, single cell hairs that project strongly from the leaf surface (e.g., *Oplismenus hirtellus*; Fig. 4F), increase leaf-boundary layer resistance and potentially reduce transpiration in more arid environments (e.g., Haworth and McElwain, 2008). They can also provide mechanical protection (saw-teeth) along the leaf edge as with *P. sieberiana* (Fig. 4D). In certain cases when trichome cells are lost (particularly for fossil specimens), a rosette of cells remains to pinpoint a trichome base, exemplified by *S. amazonia* (see arrow in Fig. 4C). Degree of cell wall undulation varies greatly among species, and can indicate the position of the leaf in the canopy (Kürschner, 1997). Cells on individual leaves growing in shade are larger and can be more undulated (puzzle-piece shaped) than those in direct sunlight (Kürschner, 1997), such as those on *L. nobilis* (Fig. 4A). Papillae (micro-scale protrusions; Fig. 4H) are also a common micromorphological ornamentation on the leaf surface, and are particularly abundant on modern and fossil species of *Ginkgo* (Figs. 4H and 5C, 5F, 5J). They help to create a superhydrophobic surface (Johnson and Dettre, 1964) that sheds water to eliminate the growth of epiphyllous species (Barclay et al., 2013), and which can also help to remove particulate matter in the process (Barthlott, 1977). The papillae can also obscure the sunken stomata beneath them making it difficult to characterize the size and shape of

these stomata. Our techniques allow for imaging of subsurface features which can bypass this issue.

We focused on *Ginkgo* as our archetypical species for preparation and imaging comparisons because of its prominence in paleoenvironmental reconstruction. The leaf morphology of the genus *Ginkgo* has remained relatively unchanged since the Late Cretaceous, and is often used to reconstruct pCO_2 based on stomatal index (Lomax and Fraser, 2015; Roth-Nebelsick, 2005). The most striking results of this study are the images procured from the Eocene and Cretaceous cuticles from *G. adiantoides*. The use of confocal with Airyscan capacity (Figs. 5A and 5D) produced images of much greater quality when compared to images created using widefield fluorescence (Figs. 5G–5I). Airyscan also allowed for realistic three-dimensional renderings of the cuticle surface (Figs. 5B and 5E). The Airyscan images of the early Eocene specimens show superb preservation of venation, the arrangement of epidermal cells, and the location and size of the stomatal pore. The quality of the Airyscan imaging (Figs. 5C and 5F) over widefield fluorescence (Fig. 5I) is even more evident at the higher levels of magnification. The images taken at high magnification under widefield fluorescence become swamped by backscatter, making features difficult to image. The greater clarity of Airyscan allows clear resolution of the papillae protruding over the stomatal pore, as well as epidermal papillae. These are both features that help to prevent wetting of the leaf surface, increasing photosynthetic productivity, and are features found on modern *G. biloba* (Fig. 5J). The Cretaceous samples also have clearly defined epidermal features, with bifurcating veins, defined stomatal pores, and clearly visible cell boundaries in interveinal areas. However, these older fossils of *G. adiantoides* have fewer epidermal papillae and papillae that less strongly arch over the stomatal pore, making them somewhat less similar to the modern species of *G. biloba*.

The protocol presented in this study presents a viable option to efficiently produce robust long-term mounts of intact herbarium and fossil leaf specimens. The flowchart in Figure 6 provides a good starting point for researchers interested in utilizing our protocol. The specimens can then provide high fidelity images of plant cuticle surface and subsurface structures through the use of superresolution or traditional confocal microscopy. Our proposed methodology has wide reaching applications. Cuticle image archives could be an invaluable tool for both plant systematics and paleobotanists who could use these techniques to better identify shifts in vegetation across multiple geological time scales (e.g., Dilcher, 1974; Wooller et al., 2003). Three-dimensional images of plant cuticle would even allow for more precise quantification of stomatal density and structure, which could result in better estimates of fluctuations in pCO_2 in deep time.

ACKNOWLEDGMENTS

RSB acknowledges funding from the Smithsonian's National Museum of Natural History (Peter Buck Deep Time Fellowship and the Paleobotany Fund). Support for MAU, MS, and SWP provided by the US National Science Foundation Advances in Biological Informatics (NSF DBI-1262561 to SWP). Scott Wing and Kirk Johnson of NMNH provided fossil samples. Rusty Russell and Debbie Bell of the US National Herbarium provided permission to sample herbarium specimens. Steven Siegler also provided permission to sample herbarium specimens at the University of Illinois Herbarium. NMNH volunteer Pam Hamilton imaged *Ginkgo biloba* specimens under eSEM at the NMNH Imaging Laboratory, run by Scott Whittaker. We thank the editor of MRT and the reviewers for their comments, which helped improve the manuscript.

REFERENCES

Anderson LE. 1954. Hoyer's solution as a rapid permanent mounting medium for bryophytes. Bryologist 57:242–244.

Barclay RS, McElwain JC, Dilcher DL, Sageman BB. 2007. The cuticle database: developing an interactive tool for taxonomic and paleoenvironmental study of the fossil cuticle record. In: Jarzen DM, Manchester SR, Retallack GJ, Jarzen SA, editors. Advances in angiosperm paleobotany and paleoclimatic reconstruction—Contributions Honoring David L. Dilcher and Jack A. Wolfe, Courier Forschungsinstitut Senckenberg, Vol. 258. pp. 39–55.

Barclay RS, Wilf P, Dilcher DL, McElwain JC. 2012. The Cuticle Database Project. The Earth and Environmental Systems Institute of Pennsylvania State University; http://cuticledb.eesi.psu.edu/; version 1.1.

Barclay RS, Wing SL. 2016. Improving the *Ginkgo* CO_2 barometer: implications for the early Cenozoic atmosphere. Earth Planet Sci Lett. doi:10.1016/j.epsl.2016.01.012

Barclay RS, McElwain JC, Duckett JG, Pressel S, van Es MH, Mostaert AS, Sageman BB. 2013. New methods reveal oldest known fossil epiphyllous moss: *Bryiidites utahensis* gen. et sp. nov. (Bryidae). Am J Bot 100:2450–2457.

Barthlott WEN. 1977. Raster-Elektronenmikroskopie der Epidermis-Oberflächen von Spermatophyten. Tropische und subtropische Pflanzenwelt (Akad. Wiss. Lit. Mainz) 19:367–465.

Beerling DJ, McElwain JC, Osborne CP. 1998. Stomatal responses of the 'living fossil' *Ginkgo biloba* L. to changes in atmospheric CO_2 concentrations. J Exp Bot 29:1603–1607.

Beerling DJ, Royer DL. 2011. Convergent cenozoic CO_2 history. Nat Geosci 4:419–420.

Berleth TJG. 1993. The role of monopteros gene in organizing the basal body region of Aradopsis embryo. Development 118:575–587.

Brown PA. 1997. A review of techniques used in preparation, curation and conservation of microscope slides at the Natural History Museum, London. Biol Curator 10:1–33.

Cleal CJ, Zodrow EL. 1989. Epidermal structure of some medullosan *Neuropteris* foliage from the Middle and Upper Carboniferous of Canada and Germany. Palaeontology 32:837–882. [Patternmatch]

Cleal CJ, Shute CH. 2007. The effect of drying on epidermal cell parameters preserved on plant cuticles. Acta Palaeobot 47:315–326.

Da Silva G, Serrano R, Teixeira Gomes E, Silva O. 2015. Botanical features for identification of *Gymnosporia arenicola* dried leaf. Microscopy Res Tech 79:1001–1009.

Dilcher DL. 1974. Approaches to the identification of fossil leaf remains. Bot Rev 40:1–157.

Dring DM. 1955. A periodic acid-Schiff technique for staining fungi in higher plants. New Phytol 54:277–279.

Dunn RE, Strömberg CAE, Madden RH, Kohn MJ, Carlini AA. 2015. Linked canopy, climate and faunal evolution in the Cenozoic of Patagonia. Science 347:258–261.

Feldman AT, Dapson RW. 1981. Comparison of the intensity of fluorescence of various mounting media. J Histotechnol 4:71–72.

Gilme JM and Wagner DH. 2013. Laboratory techniques: Slide preparation and stains. In: Glime JM, editor. Bryophyte ecology, Vol. 3. Methods. Michigan: Michigan Technological University. pp. 2-2–1-30.

Haworth M, McElwain J. 2008. Hot, dry, wet, cold or toxic? Revisiting the ecological significance of leaf and cuticular micromorphology. Palaeogeogr Palaeoclimatol Palaeoecol 262:79–90.

Johnson RE, Dettre RH. 1964. Contact angle hysteresis. III. Study of an idealized heterogeneous surface. J Phys Chem 68:1744–1750.

Jones KH, Senft JA. 1985. An improved method to determine cell viability by simultaneous staining with fluorescein diacetate-propidium iodide. Journal of Histochemistry and Cytochemistry 33:77–79.

Klingman AM, Mescon H. 1950. The periodic acid-Schiff stain for demonstrantion of fungi in animal tissue. J Bacteriol 60:415–412.
Kouwenberg LLR, Kürschner WM, McElwain JC. 2007. Stomatal frequency change over altitudinal gradients: prospects for paleoaltimetry. Rev Minerol Geochem 66:215–241.
Kovar-Eder J, Kvacek Z, Meller B. 2001. Comparing Early to Middle Miocene floras and probable vegetation types of Oberdorf N Voitsberg (Austria), Bohemia (Czech Republic), and Wackersdorf (Germany). Rev Palaeobot Palynol 114:83–125.
Kürschner WM. 1997. The anatomical diversity of recent and fossil leaves of the durmast oak (*Quercus petraea* Lieblein/*Q. pseudocastanea* Goeppert) implications for their use as biosensors of palaeoatmospheric CO_2 levels. Rev Palaeobot Palynol 96:1–30.
Kürschner WM, Kvaček Z, Dilcher DL. 2008. The impact of Miocene atmospheric carbon dioxide fluctuations on climate and the evolution of terrestrial ecosystems. Proc Natl Acad Sci USA 105: 449–453.
Lomax BH, Fraser WT. 2015. Palaeoproxies: Botanical monitors and recorders of atmospheric change. Palaeontology 58:759–766.
Palmer PG, Tucker AE. 1981. A scanning electron microscope survey of the epidermis of Eart African grasses: I. Smithsonian Contrib Bot 49:1–84.
Retallack GJ. 2001. A 300-million-year record of atmospheric carbon dioxide from fossil plant cuticles. Nature 411:287–290.
Roth-Nebelsick A. 2005. Reconstructing atmospheric carbon dioxide with stomata: Possibilities and limitations of a botanical pCO_2 sensor. Trees 19:251–265.
Ruzin SE. 1999. Plant Microtechnique and Microscopy. New York: Oxford University Press. New York. 336 p.
Sivaguru M, Fried GF, Sivaguru BS, Sivaguru VA, Lu X, Cho KH, Saif MTA, Lin B, Sadayappan S. 2015. Cardiac muscle organization revealed in 3D by imaging whole-mount mouse hearts using two-photon fluorescence and confocal microscopy. Biotechniques 59: 295–308.
Sivaguru M, Urban MA, Fried G, Wesseln CJ, Mander L, and Punyasena SW. 2016. Imaging nanoscale pollen morphology with superresolution structured illumination and Airyscan microscopy. Microsc Res Tech (special issue).
Solga A, Cerman Z, Striffler BF, Spaeth M, Barthlott W. 2007. The dream of staying clean: Lotus and biomimetic surfaces. Bioinspir Biomimet 2:S126–S134.
Stockey RA, Frevel BJ. 1997. Cuticle micromorphology of *Prumnopitys philippi* (Podocarpaceae). Int J Plant Sci 158:198–221.
Stockey RA, Frevel BJ, Woltz P. 1998. Cuticle micromorphology of Podocarpus: Section Scytopodium (Podocarpaceae) of Madagascar and South Africa. Int J Plant Sci 159:923–940.
Strömberg CAE. 2011. Evolution of grasses and grassland ecosystems. Ann Rev Earth Planet Sci 39:517–544.
Van der Burgh J, Visscher H, Dilcher DL, Kürschner WM. 1993. Paleoatmospheric signatures in Neogene fossil leaves. Science 260: 1788–1790.
Villani TS, Koroch AR, Simon JE. 2013. An improved clearing and mounting solution to replace chloral hydrate in microscopic applications. Appl Plant Sci 1:1–5.
Weisshart K. 2014. The basic principle of Airyscanning. Zeiss Technology Note. pp. 22.
Willis K, McElwain J. 2013. The evolution of plants. Gosport, UK: Oxford University Press. pp. 425.
Woodward FI. 1987. Stomatal numbers are sensitive to increases in CO_2 from preindustrial levels. Nature 327:617–618.
Wooller MJ, Swain DL, Ficken KJ, Agnew DQ, Street-Perrott FA, Eglinton G. 2003. Late Quaternary vegetation changes around Lake Rutundu, Mount Kenya, East Africa: Evidence from grass cuticles, pollen and stable carbon isotopes. J Quat Sci 18:3–15.